Published in final edited form as:

Neuroscience. 2015 October 1; 305: 15–25. doi:10.1016/j.neuroscience.2015.07.069.

High-gamma band fronto-temporal coherence as a measure of functional connectivity in speech motor control

Johnathan Kingyon[1], **Roozbeh Behroozmand**[3,4], **Ryan Kelley**[3], **Hiroyuki Oya**[3], **Hiroto Kawasaki**[3], **Nandakumar S. Narayanan**[1,2,*], and **Jeremy D. W. Greenlee**[3,*]

[1]Department of Neurology, University of Iowa, Iowa City, IA

[2]Aging Mind and Brain Initiative, Carver College of Medicine, University of Iowa, Iowa City, IA

[3]Department of Neurosurgery, University of Iowa, Iowa City, IA

[4]Department of Communication Sciences and Disorders, University of South Carolina, Columbia, SC

Abstract

The neural basis of human speech is unclear. Intracranial electrophysiological recordings have revealed that high-gamma band oscillations (70–150 Hz) are observed in frontal lobe during speech production and in the temporal lobe during speech perception. Here, we tested the hypothesis that the frontal and temporal brain regions had high-gamma coherence during speech. We recorded electrocorticography (ECoG) from the frontal and temporal cortices of five humans who underwent surgery for medically intractable epilepsy, and studied coherence between frontal and temporal cortex during vocalization and playback of vocalization. We report two novel results. First, we observed high-gamma band as well as theta (4–8 Hz) coherence between frontal and temporal lobes. Second, both high-gamma and theta coherence were stronger when subjects were actively vocalizing as compared to playback of the same vocalizations. These findings provide evidence that coupling between sensory-motor networks measured by high-gamma coherence plays a key role in feedback-based monitoring and control of vocal output for human vocalization.

Keywords

Auditory cortex; Premotor cortex; LFP; speech; efference copy; ECoG

Corresponding Authors: Nandakumar Narayanan, nandakumar-narayanan@uiowa.edu, Jeremy Greenlee, jeremy-greenlee@uiowa.edu, 200 Hawkins Drive, University of Iowa Hospitals and Clinics, Iowa City, IA, 52242, Fax: (319) 384-7199.
*These authors contributed equally to this work.

INTRODUCTION

Speech and language are uniquely human behaviors. The effort to define the neural circuits controlling normal and disordered speech has been limited largely to non-invasive techniques. However, in some cases direct recordings have been obtained from humans undergoing surgical treatment of medically intractable epilepsy. Because of the unique combination of temporal (i.e. milliseconds) and spatial (i.e. millimeters) resolution, these direct electrical recordings from the human cortex are particularly well-suited to investigate the neural bases of human speech.

One common pattern observed from areas that are required for language is oscillations in the high-gamma band. Specifically, high-gamma oscillations between 70 and 150 Hz are observed from inferior frontal gyrus during speech production (Flinker et al. 2010; Bouchard et al. 2013; Chang et al. 2013). Similar high-gamma oscillations have also been reliably observed in temporal cortical regions during auditory processing and in behavioral (i.e. vocal) compensation to feedback perturbation (Edwards et al. 2005; Greenlee et al. 2011, 2013). These results suggest the possibility that speech production centers in frontal cortex interact with auditory and language processing centers in the temporal lobe (Garell et al. 2013), which would be consistent with current models of speech production (Guenther et al. 2006; Houde and Nagarajan 2011).

Here, we test the hypothesis that frontal and temporal cortices interact via coherence in the high-gamma band as compared to the theta band. This idea predicts that high-gamma coherence should be modulated by vocalization. We studied this issue in five human patients undergoing surgery for treatment of medically intractable epilepsy. We report two new findings: 1) we observed specific high-gamma (70–150 Hz) coherence between superior temporal gyrus (STG) and frontal cortex, and 2) high-gamma coherence was stronger when subjects were actively vocalizing, particularly for contacts in inferior frontal gyrus (IFG), as compared to playback conditions. These data provide insight into how frontal and temporal cortices interact to control speech production.

METHODS

Subjects

Five males (ages 23–47 years, mean 32) from a larger pool of subjects undergoing surgical treatment of medically intractable epilepsy met criteria for this study. All subjects underwent pre-operative neuropsychological testing which confirmed normal language functions. All subjects were right-handed with left-lateralized language hemispheric dominance based on pre-operative Wada testing. All subjects had left-sided frontal, temporal, and Heschl's gyrus recording electrodes. Written informed consent was obtained from every subject and all research protocols were approved by the University of Iowa Human Subjects Review Board. Experiments were conducted in a specially designed and electromagnetically-shielded private subject suite in the University of Iowa General Clinical Research Unit. Subjects did not incur any additional medical or surgical risks by participating in this study.

All subjects completed an extensive pre-surgical assessment which included a detailed neurological examination, brain imaging (MRI, PET, and SPECT), and a neuropsychological evaluation that confirmed normal speech and language functions. No anatomic lesions were observed in the cortical regions of interest to this study in any subject. Audiometric testing was conducted and all subjects were found to have normal hearing.

Electrode Implantation

Detailed descriptions of the Heschl's gyrus hybrid depth electrode (HDE; Ad-Tech, Racine, WI) used in this study and the methods of electrode implantation and subsequent anatomical localization of recording sites have been presented in earlier studies from our laboratory (e.g. Howard et al. 1996, 2000; Brugge et al. 2008; Reddy et al. 2010). HDEs were guided stereotactically (Stealth, Medtronic, Minneapolis, MN) roughly parallel to the long axis of the left Heschl's gyrus. Each HDE carried 4 or 6 macro-contacts spaced 1 cm apart and 14 micro-contacts spanning the length of the HDE that consisted of 40-μm wires with exposed ends protruding 0.5 mm from the electrode shaft. Custom manufactured high-density surface electrode arrays were also placed on the exposed peri-Sylvian and frontal and prefrontal cortex. The peri-Sylvian and frontal/prefrontal surface recording arrays consisted of 96 and 32 platinum-iridium disc electrodes, respectively, embedded within a silicon sheet (Ad-Tech, Racine, WI). Inter-contact spacing for the peri-Sylvian arrays was 5 mm center-to-center and 3 mm contact diameter. The frontal/prefrontal grids utilized 10 mm center-to-center spacing. The exact position of the recording arrays differed somewhat between subjects as placement was based on subject-specific clinical considerations. In all subjects, the coverage provided by the arrays included significant portions of the lateral STG, including a previously described posterior lateral superior temporal auditory area (Howard et al. 2000). The electrodes remained in place during a 14-day hospital stay during which the subjects underwent continuous video-EEG monitoring. EEG monitoring confirmed that the cortical areas pertinent to this study did not show abnormal interictal activity. None of these areas were part of the epileptogenic focus and its eventual resection.

Electrode Localization

The position of each recording electrode was localized using a combination of high-resolution digital photographs taken intra-operatively during electrode placement and removal, as well as thin-cut pre- and post-implantation MRI (0.78 × 0.78 × 1.0 mm voxel size) and CT (0.45 × 0.45 × 1.0 mm voxel size) scans. Pre- and post-implantation CT and MRIs were co-registered using a 3-D rigid-fusion algorithm implemented in FMRIB's Linear Image Registration Tool (Jenkinson et al. 2002). Coordinates for each electrode obtained from post-implantation MRI volumes were transferred to pre-implantation MRI volumes. The location of every contact relative to visible surrounding brain structures was compared in both pre- and post-implantation MRI volumes. The resultant electrode locations were then mapped to a 3-D rendering of the supratemporal plane for Heschl's gyrus electrodes and lateral surface for the grids. The estimated overall error in electrode localization using these techniques does not exceed 2 mm based on visual inspection.

Experimental Design

Each experiment consisted of two blocks of vocalization and two blocks of listening to the playback of the same self-produced vocalizations. During the vocalization task, subjects were asked to maintain a steady vocalization of the vowel sound /a/ for approximately 2 seconds at their conversational pitch and volume. This vocal task was repeated 30–50 times during each block with subjects taking short breaks (1–2 seconds) between successive utterances and vocalizing at their own pace. A 10 dB gain (Mark of the Unicorn, Cambridge, MA) was added to the voice signal such that this resultant auditory feedback signal would partially mask the effect of air-borne and bone-conducted feedback. At conversational levels, subjects maintained their voice volume at about 70–75 dB and received their feedback (through inset earphones) at 80–85 dB in vocalization blocks. Subjects wore earphones during the entire experiment.

Electrophysiological Recording

Research recordings were initiated several days post-implantation after subjects had fully recovered from implantation surgery. The ECoG signals were simultaneously acquired with voice and feedback signals using a multi-channel data acquisition system (System3, Tucker-Davis Technologies, Alachua, FL) under both vocalization and playback conditions. Electrodes were referenced to an extracranial subcutaneous electrode near the vertex. The ECoG signals were band-pass filtered (1.6–1000 Hz, −12dB/octave anti-aliasing filter) and then digitized with a sampling frequency of 2034.5 Hz. Digitized data were then resampled offline at 2 kHz (MATLAB, Natick, MA) for further processing.

ECoG Data Analysis

Recordings from all Heschl's gyrus and lateral grid electrodes were inspected to ensure they were not contaminated by epileptiform activity or artifact and power line noise was removed using an adaptive notch-filtering procedure. Local field potentials, time-frequency (event-related band power; ERBP) responses, and coherence calculations were computed using the EEGLAB and Neurospec toolboxes and custom-written MATLAB routines (Rosenberg et al. 1989; Halliday et al. 1998; Delorme and Makeig 2004; Narayanan and Laubach 2009; Narayanan et al. 2013).

Local field potentials were filtered using the EEGLAB function *eegfilt*.m and time-frequency spectrograms were obtained using the EEGLAB function *newtimef.m*, with which power spectral density in the high-gamma band was obtained using fast Fourier transform (FFT) with sliding window of 128 ms long (256 points at 2 kHz) with 2.5 ms sliding step, and frequency resolution of 3.9063 Hz. For each trial, 200 ms prior to voice onset to 350 ms after voice onset were analyzed. The short post-onset time window was required due to feedback changes that were introduced into auditory feedback during vocalization as part of other experimental protocols. We further cut each epoch to −100 to +250 ms from voice onset and frequency range between 4 and 160 Hz to avoid windowing artifact. Baseline periods were chosen from −100 to 0 ms. Power was normalized to decibels using the formula: $\log10(\text{Power}_{freq} / \text{Power}_{baseline})$. The single trial spectral power time series were then averaged over the total number of trials for vocalization and playback conditions separately and results were represented as time-frequency plots of power for each individual

contact. We considered the high-gamma band as the frequency range from 70 to 150 Hz (e.g. Greenlee et al. 2011, 2013) and the theta band as 4–8 Hz.

Coherence Analysis

Coherence was used to measure the consistency of phase values and changes in this consistency over a peri-stimulus time window for a given frequency band between two different recording sites (Halliday et al. 1998; Narayanan et al. 2013). Coherence was performed using the Neurospec toolbox (Rosenberg et al. 1989). Coherence and phase between two continuously varying signals from two distinct ECoG contacts was calculated using type '2' analysis with the Neurospec function *sp2a2_m1*. Inter-site coherence was calculated according to the formula: $|R|^2 = |f_{XY}|^2/(f_{XX})*(f_{YY})$, where f_{XX} and f_{YY} refer to the auto-spectral power densities of Fourier transformed ECoG signals recorded at site X and site Y respectively, f_{XY} refers to the cross power spectral density between X and Y, and $|R|^2$ indicates cross-spectral coherence between X and Y (equation 3.11 in Rosenberg et al. 1989). A coherence value of 0 indicates random phase at that time-frequency point between sites, and 1 indicates constant or stable phase at that time-frequency point between sites. Theta coherence was calculated with sliding windows of 256 ms (512 points at 2 kHz), shifting by increments of 25 ms, resulting in 3.9063 Hz frequency resolution. High-gamma coherence required distinct parameters and was calculated with sliding windows of 128 ms (256 points at 2 kHz), shifting by increments of 2.5 ms, resulting in 7.8125 Hz frequency resolution. Coherence analysis can be performed across any frequency range, up to Nyquist frequency, in our case up to 1 kHz. We initially examined coherence for frequencies from 1–300Hz, but as demonstrated subsequently in the results section, the strongest observed coherence occurred in and below the high-gamma range.

Accordingly, we evaluated coherence beginning 100 ms prior to and extending 250 ms after voice onset. This 350 ms analysis window did not encroach upon the end of the preceding utterance. As shown in the results section, the largest increase in coherence in the time domain occurred within 250 ms of both voice onset during speaking and playback; therefore, we utilized a time window of 0–250 ms after stimulus (i.e. voice) onset for examining the anatomical distribution of peri-stimulus coherence changes across all grid contacts.

Statistical significance of coherence was determined based on 95% confidence intervals (Rosenberg et al. 1989) verified by permutation testing (10^7 permutations) time-frequency plots or trial order. Multiple comparisons were corrected via a Bonferroni correction for family-wise error and a p value of 0.005 was determined to be significant. Significance was determined across contacts by a chi-squared test, and between conditions (i.e., vocalization, playback) via ANOVA.

Phase analysis

To determine if there was a non-random phase shift in ECoG signals between brain areas and evaluate for the possibility of a common subcortical input underlying coherence, we performed phase analyses. For each subject, average phase across either vocalization or playback trials was extracted using the Neurospec MATLAB function *sp2a2_m1.m.* Phase

was calculated by the following formula: $\theta_{XY}(\gamma) = \arg f_{XY}(\gamma)$, where γ refers to frequency, θ_{XY} refers to cross-spectral phase, and f_{XY} refers to the cross-spectral power density between ECoG sites X and Y (equation 3.12 in Rosenberg et al. 1989). An example in that paper demonstrates if a process X is a lagged version of process Y, with lag τ, then

$f_{XY}(\gamma)=\lim_{T\to\infty}\frac{1}{2\pi T}E\left(\sum_j e^{-i\gamma(\sigma_j+\tau)}\right)\left(\sum_k e^{i\gamma\sigma_k}\right)=e^{-i\gamma\tau}f_{YY}(\gamma)$ (equation 3.14), where T is duration, and σ_j and σ_k refer to the stimulus onset times for processes X and Y, respectively. This results in $\theta_{XY}(\gamma) = -\gamma\tau$ (equation 3.15).

Rendering on MNI average brain

All individual subject electrode locations were rendered in MNI template space (ICBM152) as spheres to approximate +/− 2 mm localization error (MATLAB, Natick, MA). Contour plots were superimposed over contacts of interest on a Freesurfer MNI template brain surface ('BrainMesh_ICBM152.nv,' BrainNet Viewer MNI152 template surface, downloaded from Neuroimaging Informatics Tools and Resources Clearinghouse at http://www.nitrc.org/projects/bnv/) to generate summary plots of coherence results across all subjects (Fischl, Sereno, Tootell, et al. 1999; Desikan et al. 2006; Xia, Wang, He 2013).

RESULTS

High-gamma coherence recapitulates auditory circuits

We first evaluated our analysis of coherence between brain regions known to be functionally connected. Humans possess at least three functionally connected auditory fields, including posteromedial Heschl's gyrus, anterolateral Heschl's gyrus, and lateral STG (Howard et al. 2000; Brugge et al. 2003; Kumar et al. 2011; Nourski et al. 2012). To test our hypothesis that coherence analysis would identify these known connections, we selected one electrode in posteromedial Heschl's gyrus (Fig 1A) and one electrode on lateral STG (Fig 1C). Both of these sites demonstrated prominent ERBP auditory responses in multiple frequency bands during playback, but the largest amplitude responses were seen in the high-gamma and theta ranges (Figs. 1B, D). STG ERBP response patterns during playback were consistent with our previous reports (Greenlee et al. 2011, 2013).

We found a statistically significant increase in coherence in the high-gamma and theta bands (based on 95% confidence intervals) between these two sites beginning just after voice onset and persisting for approximately 100 ms in the case of high-gamma (Fig 1E). To further examine the nature of the observed high-gamma coherence, we examined coherence between the same posteromedial Heschl's gyrus contact and every contact on the temporal grid, averaged across the high-gamma band within 0–250 ms after voice onset. We found focally increased high-gamma coherence on lateral STG, and a more distributed pattern of strong high-gamma coherence between the posteromedial Heschl's gyrus site and cortex just superior to the lateral fissure (Fig 1F). Notably, coherence found at the top of the grid could be influenced by ventral frontal regions (such as Broca's area) or auditory processing within the sylvian fissure, including primary auditory areas.

Coherence between frontal cortex and STG

Consistent with prior reports, both theta and high-gamma activity were prominently modulated during vocalization in STG (Flinker et al. 2010; Greenlee et al. 2011). More complex patterns were observed in inferior frontal gyrus (IFG) and dorsal premotor cortex (dPMC) in our exemplary subject (L178; Fig 2). Average local field potentials of STG, dPMC and IFG are shown during vocalization for theta (Fig 2A) and high-gamma (Fig 2B). STG showed the most modulation of these three contacts within this time window. We observed significant coherence between both STG-dPMC and STG-IFG during vocalization in both the theta (Fig 2C) and high-gamma (Fig 2D) bands. STG-IFG contained stronger average coherence across trials for both frequency bands. Figures 2E and 2F illustrate that there is stronger average coherence across frontal cortex within 0–250 ms post-voice onset for theta (Fig 2E) when compared to high-gamma (Fig 2F).

We then examined if frontal and temporal sites exhibited significant coherence across five subjects. To test this idea, we calculated the average theta and high-gamma coherence between frontal and temporal sites in each contact 0–250 ms after voice or playback onset. We observed significant STG-frontal coherence during vocalization only (Fig 3; 121 of 160 significant frontal contacts for theta band, 48 of 160 for high-gamma band). Coherence during playback between STG and frontal cortex was not significant. Two broad anatomical STG-frontal coherence patterns appeared: coherence between STG and IFG, and between STG and regions of premotor cortex (dPMC; Fig 3; see Table 1 for MNI coordinates). Notably, the dPMC ROI was more complex and less focally-defined in theta band compared to the high-gamma band (Fig 3A).

High-gamma and theta coherence between temporal cortex and IFG/dPMC

If frontal-temporal coherence is involved in speech control, it should be modulated by vocalization. To test this idea, we analyzed average coherence values from significant contacts according to three comparisons: a) vocalization and playback conditions, b) IFG and dPMC frontal areas, and c) theta and high-gamma bands (Fig 4–5; Tables 2–4). Only contacts that were significant coherence during vocalization were included in the comparisons.

For both theta and high-gamma bands, we found significantly greater average coherence with temporal grid contacts coherence during vocalization compared to playback for IFG and dPMC (Table 2; Fig 6). Frontal coherence with temporal contacts trended higher for IFG compared to dPMC for both theta and high-gamma bands (Table 3; Fig 6). Theta coherence was significantly stronger than high-gamma coherence for playback conditions only (Table 4; Fig 6). Taken together, these data indicate that there is significant high-gamma and theta coherence between frontal and temporal lobes during vocalization; IFG-temporal coherence was significantly stronger compared to dPMC-temporal coherence for vocalization in the high-gamma band.

A 3-way repeated measures ANOVA measuring the effect of frequency band, frontal brain area, and vocalization on coherence with subjects as an error term revealed main effects of frequency band, frontal brain area, and vocalization, as well as significant 2-way interactions

(Table 5). No significant effect of vocalization vs. playback was observed on STG-frontal coherence.

To determine if phase-shifts between areas were non-random, trial-averaged phase values were examined around voice onset for vocalization and playback conditions in the high-gamma (Fig 7, right panels) and theta bands (Fig 7, left panels) between STG and either IFG or dPMC contacts (see also Table 1). Phase shifts were not significantly different than 0 for theta or high-gamma bands for STG-IFG or STG-dPMC (Table 6). Additionally, phase shifts were not significant between STG-IFG and STG-dPMC or between theta and high-gamma. In sum, these data provide evidence that IFG-temporal coherence was strongest for high-gamma and theta bands during vocalization and stronger in the theta band during playback when compared to the high-gamma band.

DISCUSSION

In the present study, we tested the idea that there is high-gamma coherence between auditory and frontal cortical motor regions during vocal production. Additionally, we investigated how activity in the high-gamma band compared to the theta band. We report two new results: 1) there was high-gamma coherence between frontal and temporal lobes, and 2) coherence was stronger when subjects were actively vocalizing than playback of vocalization and stronger between IFG-temporal contacts than dPMC-temporal contacts. These data illuminate a mechanism of sensorimotor top-down control of speech in humans.

Our results in Figure 1 demonstrate that high-gamma coherence as a measure of functional connectivity is concordant with other measures of functional connectivity within the temporal lobe, namely between Heschl's gyrus and STG (Brugge et al. 2003). In addition, high-gamma coherence between dPMC and STG is consistent with reported anatomical connectivity between these regions in non-human primates and functional connectivity in humans (Romanski et al. 1999; Garell et al. 2013). Furthermore, we found that the coherence between dPMC and STG was significantly stronger during vocalization compared with playback. This demonstrated that the fronto-temporal functional connectivity was modulated during vocal production.

The observations we are reporting are supported by several other lines of work. First, previous studies have suggested that anatomically connected brain regions can have coupled oscillations across different frequency bands (Porcaro et al. 2013; Vecchiato et al. 2013). Frequency-specific coherence is one way to establish interactions between different cortical and subcortical regions and provides an efficient mechanism to convey information between distant brain areas. For example, coherence in specific frequency bands can mediate task-dependent functional mechanisms and develops as cortical networks mature (Thatcher et al. 2008). Neural synchrony in the gamma band (40–70 Hz) has been reported to convey visual information (Womelsdorf et al. 2006), while synchrony in the theta range (4–8 Hz) can convey sensory-motor integration (Bland and Oddie 2001; Cavanagh et al. 2012; Narayanan et al. 2013). Secondly, many studies report modulation of auditory cortical responses during speech production (Numminen and Curio 1999; Curio et al. 2000; Gunji et al. 2001; Ford et

al. 2002; Houde et al. 2002; Kudo et al. 2004; Heinks-Maldonado et al. 2005, 2007; Eliades and Wang 2008; Flinker et al. 2010; Greenlee et al. 2011, 2013).

Some of these previous studies showed that suppression of cortical activity during vocalization (e.g. high-gamma ERBP) was confined to higher-order auditory cortex on the lateral STG. Notably, the STG contacts we selected for several analyses had some evidence of vocalization-related suppression, as represented by regions in blue, in some conditions (i.e. Figs 4–5). However, we did not find consistent patterns of other temporal contacts that had coherence with depth contacts in Heschl's gyrus as well as with frontal cortex in this dataset.

As a primary speech generation center, the inferior frontal gyrus may serve as a hub for "top-down" processing in the auditory-motor dorsal pathway proposed by authors (Rauschecker 1998; Rauschecker and Scott 2009). Prior work from ECoG data found low-frequency coherence (Chen et al. 2011) in gamma (25–50 Hz) ranges. We find coherence during vocalization in both theta and high-gamma frequency bands, with stronger fronto-temporal coherence in theta during playback (Fig 6), implying that theta band coherence may have a specific function modulating auditory areas during speech processing (Giraud et al. 2007).

High-gamma oscillations are considered to be local phenomenon generated by cortical pyramidal cells (Schmitz et al. 2001; Traub et al. 2004). It is surprising that we found coherence in high-gamma band between remote cortical areas. Long-range theta band synchronization and local cross frequency coupling (CFC) between theta oscillation and gamma oscillation have been well documented in association with many cognitive activities and also in correlation to the performance of these activities (Schroeder et al. 2008; Canolty and Knight 2010). It is plausible to think both mechanisms, i.e. long-range theta band synchronization and local theta-high-gamma band CFC, are involved in development of high-gamma band coherence between remote areas. Of note, we found time courses of coherence of theta band and high-gamma band oscillation are distinct with peaks of coherence in different timing (Fig 2C–D). This suggests possibility that different mechanisms other than long-range theta band synchrony and local theta-high-gamma CFC might be involved in development of high-gamma band coherence between remote areas. However, with current data and analysis, we cannot determine the mechanism of development of long-range high-gamma band synchronous oscillation.

High frequency activity can be used to construct cortical maps with fine spatial resolution (Bouchard et al. 2013). When this technique is paired with anatomical techniques such as diffusion-tensor imaging, maps of cortical activity can be illustrated with considerable detail. Interestingly, we found significant high-gamma coherence between contacts (particularly in dPMC) that did not have large ERBP activity. These data indicate that brain regions without strong event-related field potentials may still be engaged in processing information and guiding behavior (Narayanan and Laubach 2006, 2009). Future work will need to examine the relationship between coherence and ERBP timing and amplitude in detail, with particular attention to response and coherence modulation by task.

Our approach has several limitations. First, we apply this to a relatively small subset of patients who had sufficient electrode coverage. The electrode coverage was limited by details of our patients' epilepsy and surgical approach and did not cover all speech motor cortical areas. Study of additional subjects might clarify the variation that is evident in the five subjects' anatomical response patterns we now report. In addition, examination of right-hemisphere implanted subjects would allow comparisons of language-dominant versus non-dominant coherence patterns. Further study is needed to elucidate potential roles of different speech motor cortical regions such as ventrolateral prefrontal, premotor, motor, and supplementary motor cortices. Furthermore, our electrodes likely integrated activity from sulci and gyri, including auditory areas within the Sylvian fissure.

Finally, because coherence does not imply causality, we cannot infer directionality or direct relationships in the measures of coherence we report. Our phase analysis indicates that phase-shifts are random between both frontal and temporal areas. Phase-alignment can promote communication between brain regions or facilitate stimulus-related events (Noda et al. 2013; Mercier et al. 2015). In the present study, we do not observe consistent, significant phase relationships between areas. Another motivation for performing phase analyses is to explore common sources contributing to coherence. We find zero or random phase in both theta and high-gamma bands; thus, we cannot rule out common auditory input contributing to the coherence metrics reported here. Future techniques that take advantage of dynamic causal modeling might help address this issue, ideally coupled with detailed tractography and regional, focal inactivation during ECoG recordings.

In summary, we found stronger high-gamma and theta band coherence between frontal and temporal brain regions during vocal production and speech motor control than during playback of vocalization. Future studies will investigate the significance of such relationships in higher order speech processing modalities and in patients with deficits in auditory processing or vocal motor control. Such experiments will further help define how the human cortex is involved in language production and perception.

Acknowledgments

Funding

This work was supported by an NIDCD K23 DC009589 to JG and an NINDS K08 NS078100 to NSN.

Grants, disclaimers or sources of support

References

Bland BH, Oddie SD. Theta band oscillation and synchrony in the hippocampal formation and associated structures: the case for its role in sensorimotor integration. Behavioural brain research. 2001; 127:119–136. [PubMed: 11718888]

Bouchard KE, Mesgarani N, Johnson K, Chang EF. Functional Organization of Human Sensorimotor Cortex for Speech Articulation. Nature. 2013; 495:327–332. [PubMed: 23426266]

Brugge JF, Volkov IO, Garell PC, Reale RA, Howard MA III. Functional Connections Between Auditory Cortex on Heschl's Gyrus and on the Lateral Superior Temporal Gyrus in Humans. Journal of Neurophysiology. 2003; 90:3749–3763.

Brugge JF, Volkov IO, Oya H, Kawasaki H, Reale Ra, Fenoy A, Steinschneider M, Howard Ma. Functional localization of auditory cortical fields of human: click-train stimulation. Hearing research. 2008; 238:12–24. [PubMed: 18207680]

Canolty RT, Knight RT. The functional role of cross-frequency coupling. Trends Cogn Sci (Regul Ed). 2010; 14:506–515. [PubMed: 20932795]

Cavanagh JF, Zambrano-Vazquez L, Allen JJB. Theta lingua franca: a common mid-frontal substrate for action monitoring processes. Psychophysiology. 2012; 49:220–238. [PubMed: 22091878]

Chang EF, Niziolek Ca, Knight RT, Nagarajan SS, Houde JF. Human cortical sensorimotor network underlying feedback control of vocal pitch. Proceedings of the National Academy of Sciences of the United States of America. 2013; 110:2653–2658. [PubMed: 23345447]

Chen, C-Ma; Mathalon, DH.; Roach, BJ.; Cavus, I.; Spencer, DD.; Ford, JM. The corollary discharge in humans is related to synchronous neural oscillations. Journal of cognitive neuroscience. 2011; 23:2892–2904. [PubMed: 20946054]

Curio G, Neuloh G, Numminen J, Jousmäki V, Hari R. Speaking modifies voice-evoked activity in the human auditory cortex. Hum Brain Mapp. 2000; 9:183–191. [PubMed: 10770228]

Delorme A, Makeig S. EEGLAB: an open source toolbox for analysis of single-trial EEG dynamics including independent component analysis. J Neurosci Methods. 2004; 134:9–21. [PubMed: 15102499]

Edwards E, Soltani M, Deouell LY, Berger MS, Knight RT. High-gamma Activity in Response to Deviant Auditory Stimuli Recorded Directly From Human Cortex. Journal of Neurophysiology. 2005; 94:4269–4280. [PubMed: 16093343]

Eliades SJ, Wang X. Neural substrates of vocalization feedback monitoring in primate auditory cortex. Nature. 2008; 453:1102–1106. [PubMed: 18454135]

Flinker A, Chang EF, Kirsch HE, Barbaro NM, Crone NE, Knight RT. Single-trial speech suppression of auditory cortex activity in humans. The Journal of neuroscience : the official journal of the Society for Neuroscience. 2010; 30:16643–16650. [PubMed: 21148003]

Ford JM, Mathalon DH, Whitfield S, Faustman WO, Roth WT. Reduced communication between frontal and temporal lobes during talking in schizophrenia. Biological Psychiatry. 2002; 51:485. [PubMed: 11922884]

Garell PC, Bakken H, Greenlee JDW, Volkov I, Reale Ra, Oya H, Kawasaki H, Howard Ma, Brugge JF. Functional connection between posterior superior temporal gyrus and ventrolateral prefrontal cortex in human. Cerebral cortex (New York, NY : 1991). 2013; 23:2309–2321.

Giraud A-L, Kleinschmidt A, Poeppel D, Lund TE, Frackowiak RSJ, Laufs H. Endogenous cortical rhythms determine cerebral specialization for speech perception and production. Neuron. 2007; 56:1127–1134. [PubMed: 18093532]

Greenlee JDW, Behroozmand R, Larson CR, Jackson AW, Chen F, Hansen DR, Oya H, Kawasaki H, Howard Ma. Sensory-motor interactions for vocal pitch monitoring in non-primary human auditory cortex. PloS one. 2013; 8:e60783. [PubMed: 23577157]

Greenlee JDW, Jackson AW, Chen F, Larson CR, Oya H, Kawasaki H, Chen H, Howard Ma. Human auditory cortical activation during self-vocalization. PloS one. 2011; 6:e14744. [PubMed: 21390228]

Guenther FH, Ghosh SS, Tourville Ja. Neural modeling and imaging of the cortical interactions underlying syllable production. Brain and language. 2006; 96:280–301. [PubMed: 16040108]

Gunji A, Hoshiyama M, Kakigi R. Auditory response following vocalization: a magnetoencephalographic study. Clinical neurophysiology: official journal of the International Federation of Clinical Neurophysiology. 2001; 112:514–520. [PubMed: 11222973]

Halliday DM, Conway BA, Farmer SF, Rosenberg JR. Using electroencephalography to study functional coupling between cortical activity and electromyograms during voluntary contractions in humans. Neuroscience letters. 1998; 241:5–8. [PubMed: 9502202]

Heinks-Maldonado TH, Mathalon DH, Gray M, Ford JM. Fine-tuning of auditory cortex during speech production. Psychophysiology. 2005; 42:180–190. [PubMed: 15787855]

Heinks-Maldonado TH, Mathalon DH, Houde JF, Gray M, Faustman WO, Ford JM. Relationship of imprecise corollary discharge in schizophrenia to auditory hallucinations. Archives of general psychiatry. 2007; 64:286–296. [PubMed: 17339517]

Houde JF, Nagarajan SS. Speech production as state feedback control. Frontiers in human neuroscience. 2011; 5:82. [PubMed: 22046152]

Houde JF, Nagarajan SS, Sekihara K, Merzenich MM. Modulation of the auditory cortex during speech: an MEG study. Journal of cognitive neuroscience. 2002; 14:1125–1138. [PubMed: 12495520]

Howard, Ma; Volkov, IO.; Abbas, PJ.; Damasio, H.; Ollendieck, MC.; Granner, Ma. A chronic microelectrode investigation of the tonotopic organization of human auditory cortex. Brain research. 1996; 724:260–264. [PubMed: 8828578]

Howard, Ma; Volkov, IO.; Mirsky, R.; Garell, PC.; Noh, MD.; Granner, M.; Damasio, H.; Steinschneider, M.; Reale, Ra; Hind, JE.; Brugge, JF. Auditory cortex on the human posterior superior temporal gyrus. The Journal of comparative neurology. 2000; 416:79–92. [PubMed: 10578103]

Jenkinson M, Bannister P, Brady M, Smith S. Improved Optimization for the Robust and Accurate Linear Registration and Motion Correction of Brain Images. NeuroImage. 2002; 17:825–841. [PubMed: 12377157]

Kudo N, Nakagome K, Kasai K, Araki T, Fukuda M, Kato N, Iwanami A. Effects of corollary discharge on event-related potentials during selective attention task in healthy men and women. Neuroscience research. 2004; 48:59–64. [PubMed: 14687881]

Kumar S, Sedley W, Nourski KV, Kawasaki H, Oya H, Patterson RD, Howard MA, Friston KJ, Griffiths TD. Predictive Coding and Pitch Processing in the Auditory Cortex. Journal of Cognitive Neuroscience. 2011; 23:3084–3094. [PubMed: 21452943]

Mercier MR, Molholm S, Fiebelkorn IC, Butler JS, Schwartz TH, Foxe JJ. Neuro-oscillatory phase alignment drives speeded multisensory response times: an electro-corticographic investigation. J Neurosci. 2015; 35:8546–8557. [PubMed: 26041921]

Narayanan NS, Cavanagh JF, Frank MJ, Laubach M. Common medial frontal mechanisms of adaptive control in humans and rodents. Nature neuroscience. 2013

Narayanan NS, Laubach M. Top-down control of motor cortex ensembles by dorsomedial prefrontal cortex. Neuron. 2006; 52:921–931. [PubMed: 17145511]

Narayanan NS, Laubach M. Methods for studying functional interactions among neuronal populations. Methods Mol Biol. 2009; 489:135–165. [PubMed: 18839091]

Noda T, Kanzaki R, Takahashi H. Stimulus phase locking of cortical oscillation for auditory stream segregation in rats. PLoS ONE. 2013; 8:e83544. [PubMed: 24376715]

Nourski KV, Steinschneider M, Oya H, Kawasaki H, Jones RD, Howard MA. Spectral Organization of the Human Lateral Superior Temporal Gyrus Revealed by Intracranial Recordings. Cerebral cortex (New York, NY: 1991). 2012

Numminen J, Curio G. Differential effects of overt, covert and replayed speech on vowel-evoked responses of the human auditory cortex. Neurosci Lett. 1999; 272:29–32. [PubMed: 10507535]

Porcaro C, Coppola G, Pierelli F, Seri S, Di Lorenzo G, Tomasevic L, Salustri C, Tecchio F. Multiple frequency functional connectivity in the hand somatosensory network: an EEG study. Clinical neurophysiology: official journal of the International Federation of Clinical Neurophysiology. 2013; 124:1216–1224. [PubMed: 23306037]

Rauschecker JP. Cortical control of the thalamus: top-down processing and plasticity. Nat Neurosci. 1998; 1:179–180. [PubMed: 10195140]

Rauschecker JP, Scott SK. Maps and streams in the auditory cortex: nonhuman primates illuminate human speech processing. Nat Neurosci. 2009; 12:718–724. [PubMed: 19471271]

Reddy CG, Dahdaleh NS, Albert G, Chen F, Hansen D, Nourski K, Kawasaki H, Oya H, Howard MA 3rd. A method for placing Heschl gyrus depth electrodes. J Neurosurg. 2010; 112:1301–1307. [PubMed: 19663547]

Romanski LM, Bates JF, Goldman-Rakic PS. Auditory belt and parabelt projections to the prefrontal cortex in the rhesus monkey. The Journal of comparative neurology. 1999; 403:141–157. [PubMed: 9886040]

Rosenberg JR, Amjad AM, Breeze P, Brillinger DR, Halliday DM. The Fourier approach to the identification of functional coupling between neuronal spike trains. Prog Biophys Mol Biol. 1989; 53:1–31. [PubMed: 2682781]

Schmitz D, Schuchmann S, Fisahn A, Draguhn A, Buhl EH, Petrasch-Parwez E, Dermietzel R, Heinemann U, Traub RD. Axo-axonal coupling. a novel mechanism for ultrafast neuronal communication. Neuron. 2001; 31:831–840. [PubMed: 11567620]

Schroeder CE, Lakatos P, Kajikawa Y, Partan S, Puce A. Neuronal oscillations and visual amplification of speech. Trends Cogn Sci (Regul Ed). 2008; 12:106–113. [PubMed: 18280772]

Thatcher RW, North DM, Biver CJ. Development of cortical connections as measured by EEG coherence and phase delays. Human brain mapping. 2008; 29:1400–1415. [PubMed: 17957703]

Traub RD, Bibbig A, LeBeau FEN, Buhl EH, Whittington MA. Cellular mechanisms of neuronal population oscillations in the hippocampus in vitro. Annu Rev Neurosci. 2004; 27:247–278. [PubMed: 15217333]

Vecchiato G, Susac A, Margeti S, De Vico Fallani F, Maglione AG, Supek S, Planinic M, Babiloni F. High-resolution EEG analysis of power spectral density maps and coherence networks in a proportional reasoning task. Brain topography. 2013; 26:303–314. [PubMed: 23053602]

Womelsdorf T, Fries P, Mitra PP, Desimone R. Gamma-band synchronization in visual cortex predicts speed of change detection. Nature. 2006; 439:733–736. [PubMed: 16372022]

HIGHLIGHTS

- We study the neural basis of human speech using intracranial electrophysiology.
- We show high-gamma band coherence (70–150 Hz) between frontal and temporal regions.
- High-gamma band coherence is stronger when patients were vocalizing.
- These results provide evidence of sensory-motor coupling during speech.

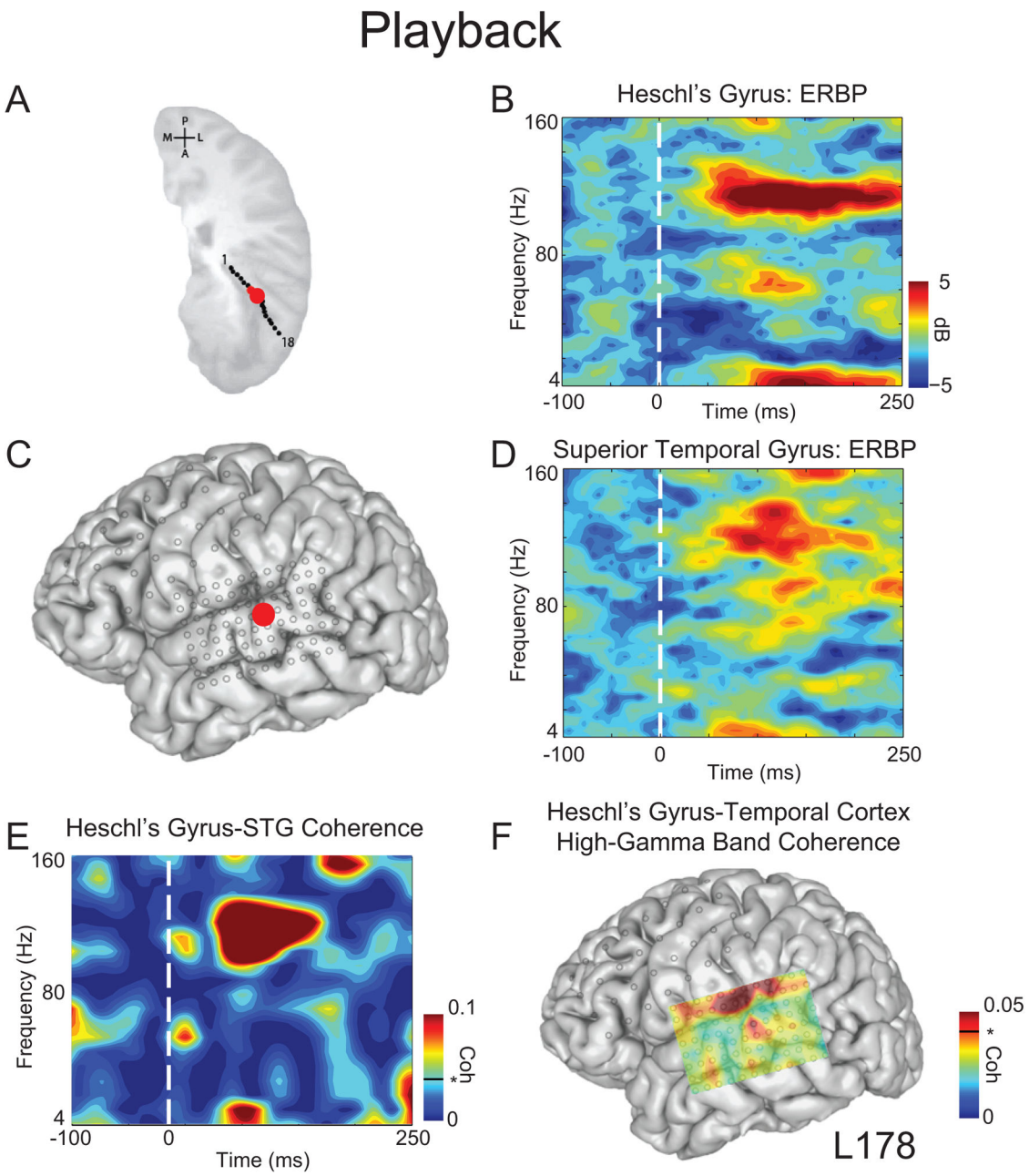

Figure 1.

Coherence between Heschl's gyrus and superior temporal gyrus during playback. A) Depth contacts in Heschl's gyrus; selected contact in red. B) Event-related band power (ERBP) for Heschl's depth contact demonstrated low frequency and high-gamma band (70–150 Hz) activity during playback. C) Temporal grid; STG selected contact in red. D) ERBP for STG demonstrated prominent high-gamma activity during playback. E) Coherence between Heschl's gyrus and STG was prominent in high-gamma frequencies. F) Distribution of high-gamma coherence (0–250 ms post-voice onset) between Heschl's gyrus contact and all temporal grid contacts. Coherence values above 0.04 (black line) are significant at $p < 0.05$. All time-frequency plots are aligned to voice onset.

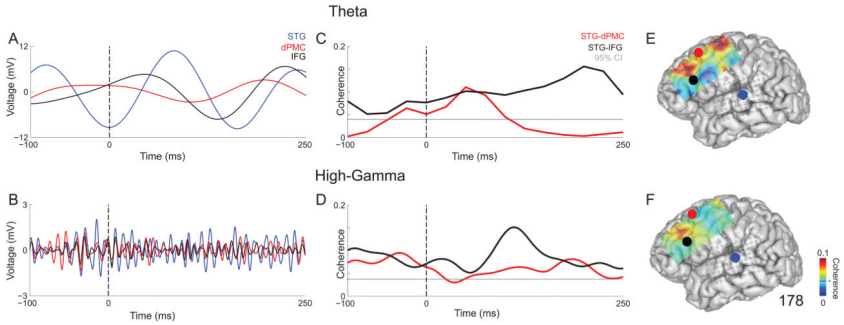

Figure 2.

Local field potentials from individual contacts in STG (blue), dorsal premotor cortex (dPMC; red), and inferior frontal gyrus (IFG; black) during vocalization from subject 178 for A) theta and B) high-gamma band. Field potentials are average across trials. Coherence for STG-dPMC (red) and STG-IFG (black) during vocalization from subject 178 for C) theta and D) high-gamma band. All time-frequency plots are aligned to voice onset. The gray line represents the 95% confidence threshold for coherence. Average coherence values for each frontal contact relative to STG from 0–250 ms post-voice onset in E) theta and F) high-gamma band. STG is shown by the blue circle, dPMC in red, and IFG in black. The 95% confidence interval for coherence is the black line on the color bar.

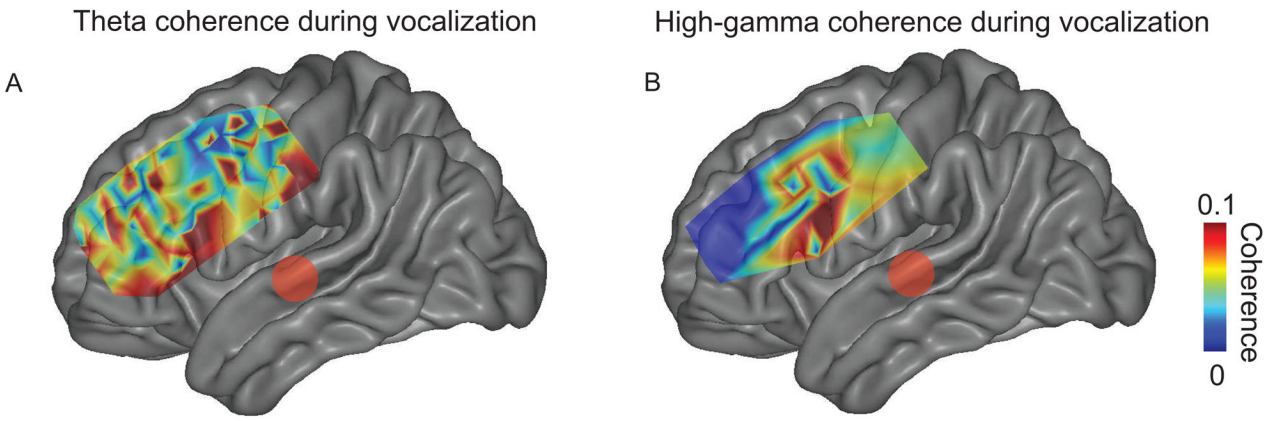

Figure 3.

Average coherence between significant frontal contacts and STG during vocalization in five subjects for theta (A) and high-gamma bands (B) 0–250 ms post-voice onset. Two major foci of coherence were seen in inferior frontal gyrus and premotor cortex. Coherence plotted only for significant contacts as determined by 95% confidence intervals on average MNI brains.

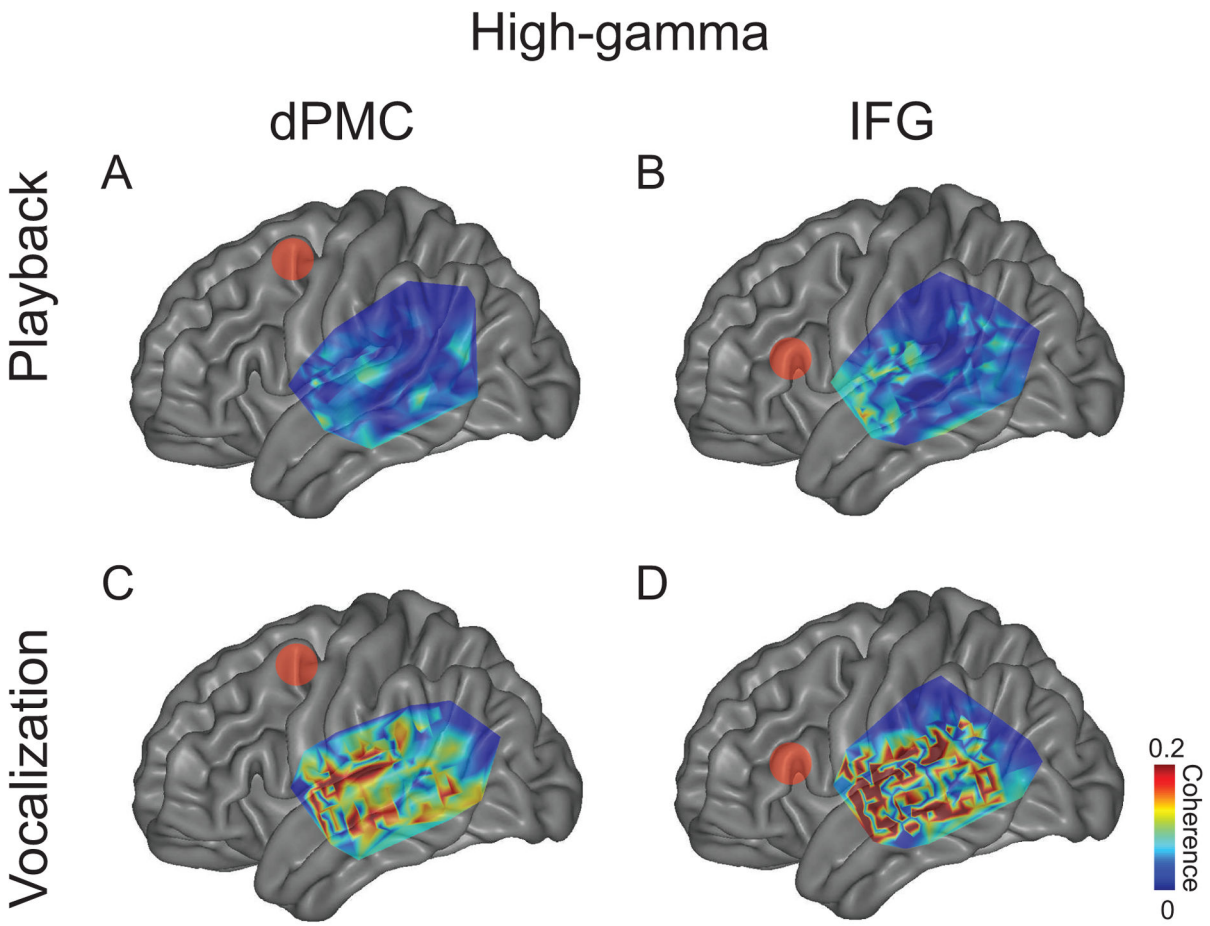

Figure 4.

Average theta coherence between frontal contacts and temporal grids. Coherence from all significant contacts is plotted for playback between temporal grids and (A) dPMC and (B) IFG and for vocalization (C–D). Red dots indicate dPMC in A and C, and IFG in B and D. All significant contacts across subjects were plotted on an average MNI brain. Coherence plotted only for significant contacts as determined by 95% confidence intervals on average MNI brains.

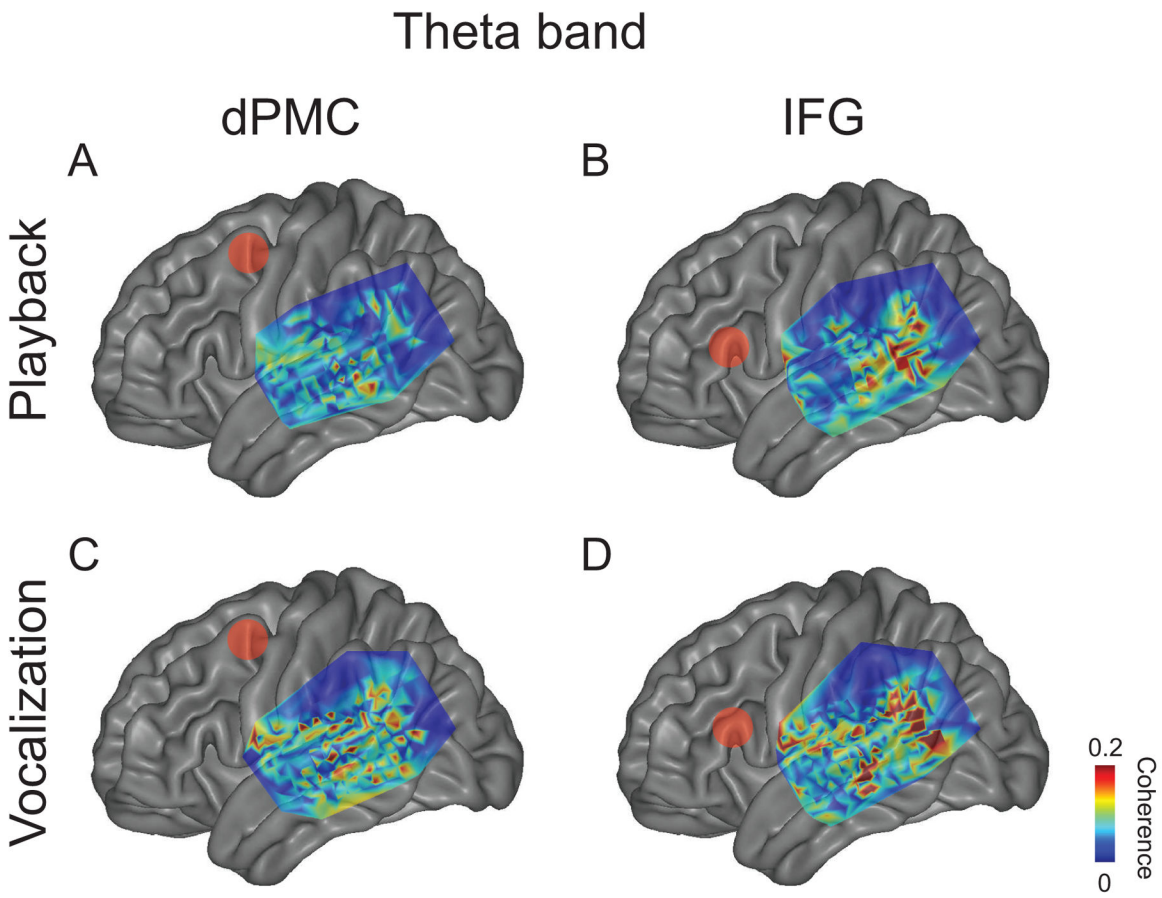

Figure 5.

Average high-gamma coherence between frontal contacts and temporal grids. Coherence from all significant contacts is plotted for playback between temporal grids and (A) dPMC and (B) IFG and for vocalization (C–D). Red dots indicate dPMC in A and C, and IFG in B and D. All significant contacts across subjects were plotted on an average MNI brain. Coherence plotted only for significant contacts as determined by 95% confidence intervals on average MNI brains.

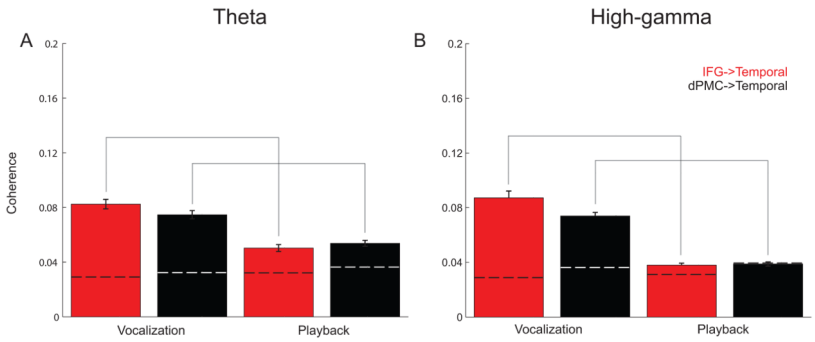

Figure 6.

Average theta and high-gamma band coherence across significant vocalization contacts in all subjects. Greater frontal-temporal coherence is observed for vocalization compared to playback, and greater frontal-temporal coherence is observed for IFG compared to dPMC. Moreover, for IFG-temporal and dPMC-temporal coherence, more theta coherence was observed during playback compared to high-gamma coherence. Frontal-temporal coherence during vocalization between theta and high-gamma bands was not statistically different. Dashed lines indicate 95% confidence intervals. Solid gray lines indicate significance via a t-test.

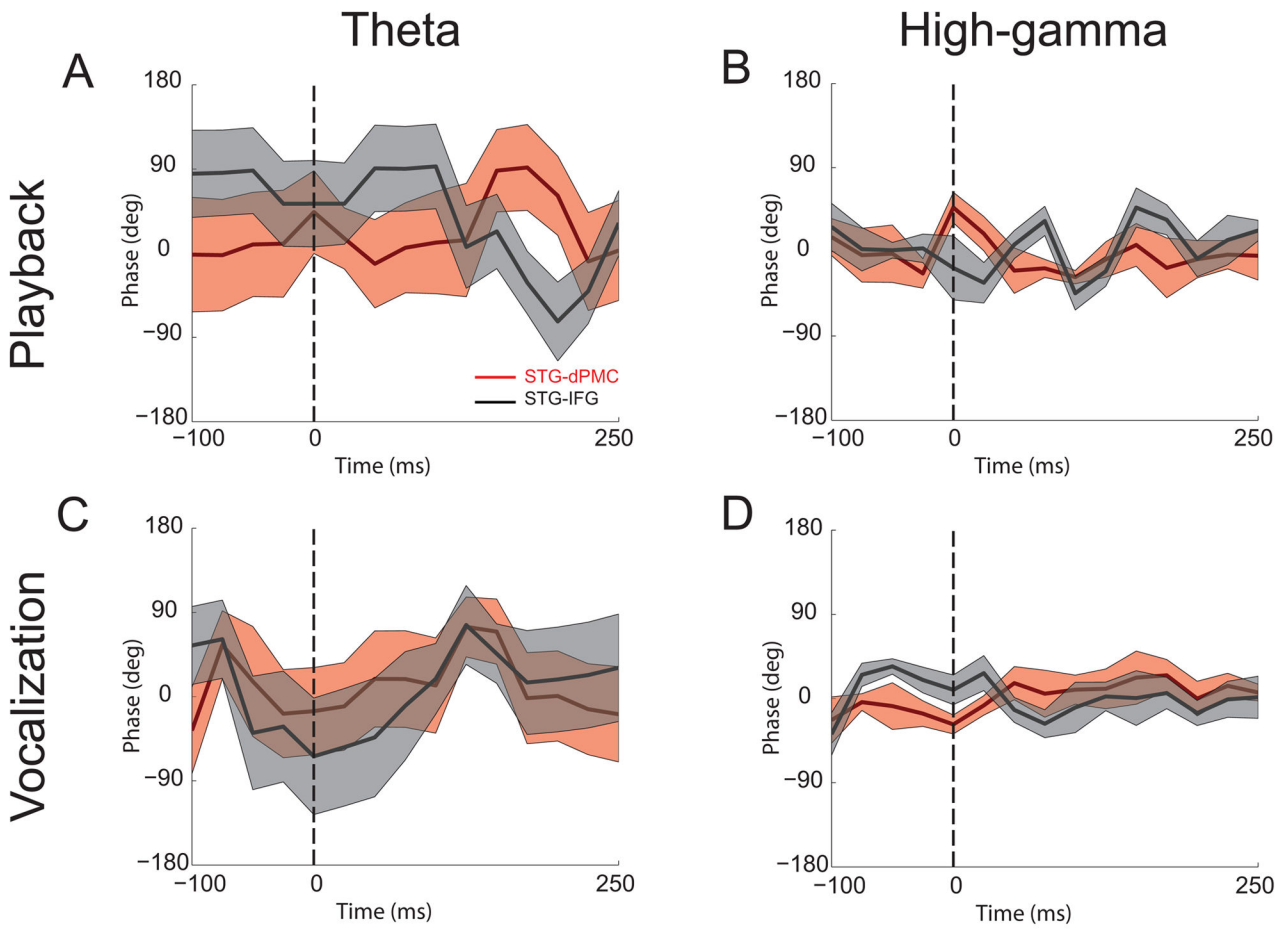

Figure 7.

Average cross-spectral phase values between STG and IFG/dPMC across subjects. Phase values were plotted for theta (A, C) and high-gamma bands (B, D) during playback and vocalization. Positive phase values indicate IFG/dPMC activity leading STG activity, while negative values indicate STG activity leading IFG/dPMC activity. Shaded regions represent standard error limits.

Table 1

MNI Coordinates across all subjects for regions of interest

Area	Subject	MNI (x)	MNI (y)	MNI (z)
STG	173	−74.1	−22.9	12.5
	178	−66.5	27.5	6.7
	206	−67.5	−22.8	7.2
	258	−65.8	−27.3	9.7
	275	−69.4	−14.2	−4.0
dPMC	173	−53.3	14.7	47.7
	178	−45.7	14.4	44.1
	206	−34.9	25.4	50.2
	258	−48.3	−2.2	55.0
	275	−58.2	1.5	34.9
IFG	173	−66.5	20.8	15.2
	178	−57.8	17.9	20.6
	206	−48.0	40.4	23.2
	258	−49.9	41.6	17.8
	275	−32.2	55.8	23.5

Table 2

Fronto-temporal coherence for vocalization vs. playback; $\alpha < 0.005$

Coherent regions	Condition	Mean coherence	Vocalization vs. playback
High-gamma			
IFG vs. temporal	Vocalization	0.08±0.005	$t = 9.4$, $p \ll 0.001$*
	Playback	0.04±0.001	
dPMC vs. temporal	Vocalization	0.07±0.003	$t = 11.5$, $p \ll 0.001$*
	Playback	0.04±0.002	
Theta			
IFG vs. temporal	Vocalization	0.08±0.004	$t = 6.3$, $p \ll 0.001$*
	Playback	0.05±0.003	
dPMC vs. temporal	Vocalization	0.07±0.003	$t = 5.6$, $p \ll 0.001$*
	Playback	0.05±0.002	

Table 3

Fronto-temporal coherence for IFG vs. dPMC; $\alpha < 0.005$

Condition	Coherent regions	Mean coherence	IFG vs. dPMC
High-gamma			
Vocalization	IFG-temporal	0.08±0.005	t = 2.0, p < 0.05
	dPMC-temporal	0.07±0.003	
Playback	IFG-temporal	0.04±0.001	t = 0.4, p > 0.7
	dPMC-temporal	0.04±0.002	
Theta			
Vocalization	IFG-temporal	0.08±0.004	t = 1.7, p < 0.1
	dPMC-temporal	0.07±0.003	
Playback	IFG-temporal	0.05±0.003	t = 0.4, p > 0.6
	dPMC-temporal	0.05±0.002	

Table 4

Fronto-temporal coherence for theta vs. high-gamma bands; $\alpha < 0.005$

Coherent Regions	Frequency Bands	Mean coherence	Theta vs. high-gamma
Playback			
IFG-temporal	Theta	0.05±0.003	$t = 5.2$, $p \ll 0.001$*
	High-gamma	0.04±0.001	
dPMC-temporal	Theta	0.05±0.002	$t = 4.5$, $p \ll 0.001$*
	High-gamma	0.04±0.002	
Vocalization			
IFG-temporal	Theta	0.08±0.004	$t = 0.8$, $p > 0.4$
	High-gamma	0.08±0.005	
dPMC-temporal	Theta	0.07±0.003	$t = 0.2$, $p > 0.8$
	High-gamma	0.07±0.003	

Table 5

Analysis of variance; $\alpha < 0.005$

Comparison	F	P
Vocalization vs. Playback	316	$p \ll 0.005$
Frequency Band (Theta vs. High-gamma)	61	$p \ll 0.005$
Frontal Area (IFG vs. dPMC)	58	$p \ll 0.005$
Vocalization & Frequency Band	28	$p < 0.005$
Vocalization & Frontal Area	7	$p < 0.009$
Frequency Band& Frontal Area	19	$p < 0.005$
3-Way interaction	1	0.28

Table 6

P-values for trial-averaged phase shifts.

	High-gamma		***Theta***	
	Vocalization	**Playback**	**Vocalization**	**Playback**
STG-dPMC vs. zero	p>0.4	p>0.5	p>0.6	p>0.6
STG-IFG vs. zero	p>0.4	p>0.4	p>0.4	p>0.2
STG-dPMC vs. STG-IFG	p>0.4	p>0.4	p>0.6	p>0.4
	STG-dPMC		***STG-IFG***	
	Vocalization	Playback	Vocalization	Playback
High-gamma vs. Theta	p>0.6	p>0.6	p>0.4	p>0.2